

Synchronization under periodic modulation of potential wells in a two-state stochastic system

Asish K. Dhara and S. R. Banerjee

Variable Energy Cyclotron Centre, 1/AF, Bidhan Nagar, Calcutta-700064, India

We analyse the effect of synchronization between noise and periodic signal in a two-state spatially extended system analytically. Resonance features are demonstrated. To have the maximum cooperation between signal and noise, it is shown that noise strength at resonance should increase linearly with the frequency of the signal. The time scale of the process at resonance is also shown to increase linearly with the period of the signal.

Noise induced large response in bistable potential to a weak periodic signal commonly referred to as stochastic resonance (SR) attracts considerable interests during recent years [1–3]. Manifestation of SR is usually exhibited as non-monotonous behavior of power spectrum of the process or as a similar behavior of the peak heights of the escape-time distribution related to switching between two wells, as a function of the noise strength [4–7]. The usage of the term "resonance" is then criticised based on two facts [8]. The value of the noise strength for which the maximum of the spectral density at forcing frequency occurs does not simply correspond to the period of the signal and for fixed noise strength, the spectral density decreases monotonically with frequency of the signal, at variance with the notion of ordinary resonance. One therefore would naturally be curious whether any characterisation of this phenomena in terms of our usual definition of resonance is possible as it was originally pictured [9].

Recently, it has been found that such description is indeed possible [10]. Simulating the continuous stochastic process into a stochastic point process with the help of an analog circuit they [10] measure the strength of the first few peaks of the residence time distribution. It is found that when strength of the first peak is plotted as a function of the frequency of the signal keeping noise strength constant, it hits a maximum for that period which is equal to twice of the inverse of the Kramers rate for the unbiased process for that particular noise strength. Alternately, when strength of the first peak is plotted as a function of noise strength it attains a maximum at that value of the noise strength for which inverse of Kramers rate for the unbiased process is equal to the period of forcing signal. Subsequently, this resonant behavior is also experimentally verified in the polarised emission of vertical cavity surface emitting laser [11]. In this paper we analyse these results analytically.

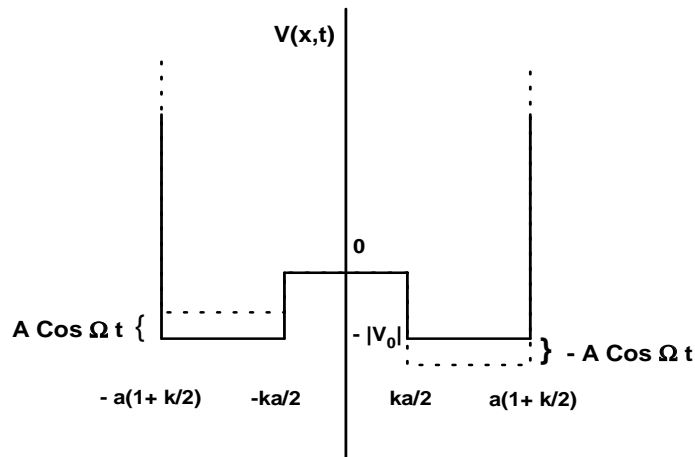


FIG. 1. Potential $V(x, t)$ at time t as a function of x .

Response of a two-state spatially extended system embedded to a noisy environment under the influence of a periodic field is of our concern. The simplest model [12] for the two-state spatially extended system is to consider a particle moving in the piecewise double well potential $V(x)$ under the influence of white noise. The potential $V(x)$ is shown in Fig.1. The influence of the external periodic field is usually described by the modulation of the potential well in the following fashion. The potential at any instant of time t for the left state is replaced by $-|V_0| + A \cos \Omega t$ and that for the right state is replaced by $-|V_0| - A \cos \Omega t$ with A, Ω

being the amplitude and frequency of the periodic signal and $|V_0|$ is the barrier height when there is no modulation.

The Fokker-Planck equation (FPE) for the probability distribution function $P(x, t)$ for position x of the particle at time t for this process is

$$\frac{\partial P(x, t)}{\partial t} = \frac{\partial}{\partial x} \left[\frac{\partial V(x, t)}{\partial x} P(x, t) \right] + D \frac{\partial^2 P(x, t)}{\partial x^2}, \quad (1)$$

where D is strength of the white noise. It is clear that for the potential in Fig.1, $\frac{\partial V}{\partial x} = 0$ everywhere except at the discontinuous points. Therefore in each region of $V(x, t) = \text{constant}$, the FPE (1) reduces to simple diffusion equation. The solution in each region are to be matched with the continuity of probability current and jump conditions at the discontinuous points $[-ka/2, ka/2]$ at each time. These conditions are to be supplemented by the reflecting boundary conditions at the walls $[-a(1 + k/2), a(1 + k/2)]$.

In this paper we however are interested in first passage time density function (FPTDF) with mean first passage time (MFPT) being a important parameter of the process. To be specific we concentrate on the events starting from $x = -1$ and ending at $x = 1$. As the potential is symmetric, the MFPT $< t(-1 \rightarrow 1) >$ would be same as $< t(1 \rightarrow -1) >$. Thus the conditions that the required solution of Eq.(1) satisfies are

$$P'(-a(1 + k/2), t) = 0, \quad (2a)$$

$$e^{[-|V_0| + A \cos \Omega t]/D} P(-ka/2 - 0, t) = P(-ka/2 + 0, t), \quad (2b)$$

$$P'(-ka/2 - 0, t) = P'(-ka/2 + 0, t), \quad (2c)$$

$$P(ka/2 - 0, t) = e^{[-|V_0| - A \cos \Omega t]/D} P(ka/2 + 0, t), \quad (2d)$$

$$P'(ka/2 - 0, t) = P'(ka/2 + 0, t), \quad (2e)$$

$$P(1, t) = 0, \quad (2f)$$

where prime over P in the above equations denote derivative with respect to x . Eq.(2a) corresponds to reflecting boundary condition for the wall at $x = -a(1 + k/2)$, Eq.(2b) and Eq.(2d) are the jump conditions at the discontinuous points $x = \pm ka/2$, Eq.(2c) and Eq.(2e) are the matching condition for continuity of probability current and Eq.(2f) is the absorbing boundary condition at $x = 1$ for the process considered.

For (A/D) small, we expand the solution in each region as

$$P(x, t) = e^{[-\frac{|V_0|}{2D} - \lambda t - (A/D)g(t)]} \psi(x) \left[1 + \sum_{m=1}^{\infty} (A/D)^m f_m(x, t) \right], \quad (3)$$

with $f_0 = 1$, and $g(t)$ being defined as

$$\begin{aligned} g(t) &= \cos \Omega t; -a(1 + k/2) \leq x \leq -ka/2, \\ &= 0; -ka/2 < x < ka/2, \\ &= -\cos \Omega t; ka/2 \leq x \leq 1. \end{aligned} \quad (4)$$

In Eq.(3), λ is some constant and $f_m(x, t)$ are functions, which are to be determined. Substituting the ansatz (3) in Eq.(1) and equating equal powers of (A/D) we obtain the following set of equations in each region:

$$\frac{\partial^2 \psi(x)}{\partial x^2} = -(\lambda/D) \psi(x), \quad (5a)$$

$$\left[\frac{\partial}{\partial t} - D \frac{\partial^2}{\partial x^2} \right] [\psi(x) f_n(x, t)] = \dot{g}(t) f_{n-1}(x, t); n = 1, 2, \dots, \quad (5b)$$

with $f_0 = \psi(x)$. For small (A/D) we keep only Eq.(5a) which is obtained after equating the terms $O(1)$. Substituting the approximate form of probability density in Eqs.(2a)-(2f) we obtain the following set of matching conditions for the functions $\psi(x)$.

$$\psi'_\mu(-a(1 + k/2)) = 0, \quad (6a)$$

$$e^{[-|V_0|]/D} \psi_\mu(-ka/2 - 0) = \psi_\mu(-ka/2 + 0), \quad (6b)$$

$$\psi'_\mu(-ka/2 - 0) = \psi'_\mu(-ka/2 + 0), \quad (6c)$$

$$\psi_\mu(ka/2 - 0) = e^{[-|V_0|]/D} \psi_\mu(ka/2 + 0), \quad (6d)$$

$$\psi'_\mu(ka/2 - 0) = \psi'_\mu(ka/2 + 0), \quad (6e)$$

$$\psi_\mu(1) = 0, \quad (6f)$$

We note that the solutions of Eqs.(6a)-(6f) are the exact eigenfunctions of the corresponding unperturbed process with associated eigenvalues λ_μ . Thus with this approximation the conditional probability for getting the particle at position x at time t when it is known to start from $x = -1$ at $t = 0$ is

$$P(x, t | -1, 0) = e^{-[V(x)-V(-1)]/2D} e^{-A[g(t)-1]/D} \sum_n e^{-\lambda_n t} \psi_n(x) \psi_n(-1) , \quad (7)$$

where the value of $V(x)$ and $g(t)$ would be taken as the respective values of the region where x falls. As ψ_n form the complete set, $P(x, t = 0+ | -1, 0) = \delta(x + 1)$ is automatically satisfied. The Eqs. (6a)-(6f) are readily solved to obtain the full set of eigenfunctions and corresponding eigenvalues. They express as

$$\psi_\mu(x) = C_\mu \cos\{k_\mu[x + a(1 + k/2)]\} ; -a(1 + k/2) \leq x < -ka/2 , \quad (8a)$$

$$= -C_\mu [e^{|V_0|/2D} \sin(k_\mu a) \sin\{k_\mu(x + ka/2)\} - e^{-|V_0|/2D} \cos(k_\mu a) \cos\{k_\mu(x + ka/2)\}] ; -ka/2 < x < ka/2 , \quad (8b)$$

$$= C_\mu [\cos(k_\mu ka) \cos\{k_\mu[x + a(1 - k/2)]\} - e^{|V_0|/D} \sin(k_\mu ka) \sin(k_\mu a) \cos\{k_\mu(x - ka/2)\} - e^{-|V_0|/D} \sin(k_\mu ka) \cos(k_\mu a) \sin\{k_\mu(x - ka/2)\}] ; ka/2 < x \leq 1 , \quad (8c)$$

where constant C_μ is determined from the normalisation condition

$$C_\mu^2 \int_{-1}^1 \psi_\mu^2(x) dx = 1 . \quad (9)$$

The corresponding eigenvalues are determined from the transcendental equation

$$\begin{aligned} & \cos(k_\mu ka) \cos\{k_\mu[1 + a(1 - k/2)]\} \\ & - e^{|V_0|/D} \sin(k_\mu ka) \sin(k_\mu a) \cos\{k_\mu(1 - ka/2)\} \\ & - e^{-|V_0|/D} \sin(k_\mu ka) \cos(k_\mu a) \sin\{k_\mu(1 - ka/2)\} = 0 . \end{aligned} \quad (10)$$

The expressions (8) and k_μ obtained from Eq.(10) are substituted in Eq.(7) with $\lambda_\mu = Dk_\mu^2$ to obtain the conditional probability $P(x, t | -1, 0)$ at any point x at time t .

The survival probability at time t , $S(t)$ can be obtained from Eq.(7) as

$$S(t) = \int_{-1}^1 P(x, t | -1, 0) dx , \quad (11)$$

and the first passage time density function (FPTDF) $g(t)$ is obtained from $S(t)$ as

$$g(t) = -\frac{dS(t)}{dt} . \quad (12)$$

Physically, $g(t)dt$ gives the probability that the particle reaches $x = 1$ for the first time in the time interval t and $t + dt$ starting from $x = -1$ at $t = 0$. As the expression of the conditional probability (7) is approximate and strictly valid for small (A/D) , we should demand the necessary physical conditions like positivity, normalisability on $g(t)$. Different moments of $g(t)$ can be readily calculated from the normalised $g(t)$ as

$$\langle t^j \rangle = \int_0^\infty t^j g(t) dt ; j = 1, 2, \dots . \quad (13)$$

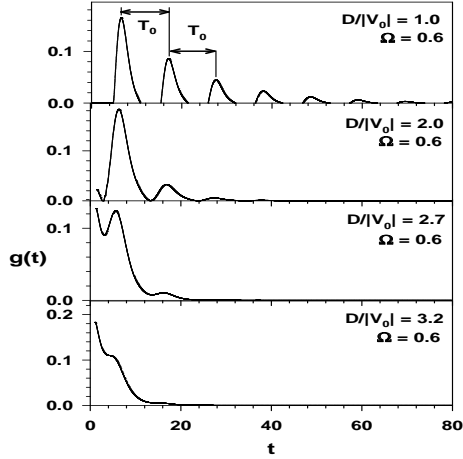


FIG. 2. FPTDF $g(t)$ as a function of t for frequency $\Omega = 0.6$ and $(D/V_0) = 1.0, 2.0, 2.7, 3.2$.

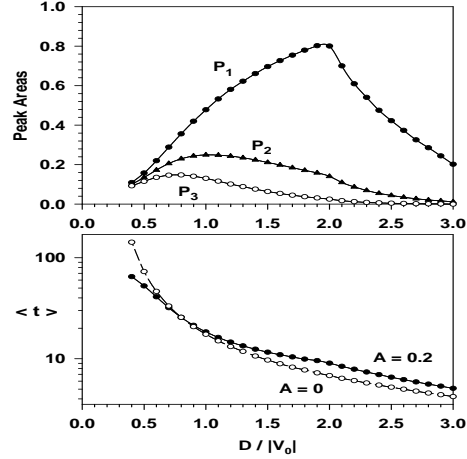


FIG. 3. Peak areas as a function of (D/V_0) and MFPT $\langle t \rangle$ as a function of (D/V_0) with signal ($A = 0.2$) [line with filled circles] and without signal ($A = 0$) [line with open circles].

The calculations are done with the potential parameters, $a = 1, k = 1, |V_0| = 0.25, A = 0.2$. Normalised FPTDF $g(t)$ as a function of t for fixed value of signal frequency $\Omega = 0.6$ and different values of $(D/|V_0|)$ are plotted in Fig.2. Multiple peaks are observed for small values of noise strength and as noise strength increases background is found dominant. $g(t)$ extends for a longer time for small noise strength. The peak heights fall exponentially with time for fixed $(D/|V_0|)$ but peak heights are increased as noise strength is lowered. Successive peaks are separated by a time exactly equal to the period of the signal frequency showing that the probability of transition is maximum after each period. At these particular times cooperation between noise and the signal in making a transition is more. It clearly demonstrates that the signal synchronizes the noise induced transition. Peak areas (counting peaks from left) are also found to be decreasing with time.

On subtracting the exponential background, the peak areas $P_n = \int g(t)dt$, where the integration is done around n th. peak are plotted as a function of $(D/|V_0|)$ in Fig.3. The figure demonstrates a non-monotonous behavior for each peak exhibiting a signature of maximum cooperation or synchronization between noise and external signal at specific value of noise strength for a particular signal frequency Ω . The position of the maximum of P_n shifts towards lower value of noise strength as peak number increases. All curves merges to low D showing at very low noise strength transition would mainly be controlled by signal most of the time.

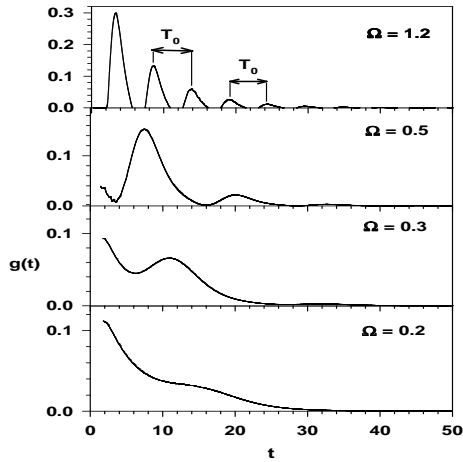


FIG. 4. FPTDF $g(t)$ as function of time t for $D/V_0 = 1.9$ and $\Omega = 0.2, 0.3, 0.5, 1.2$.

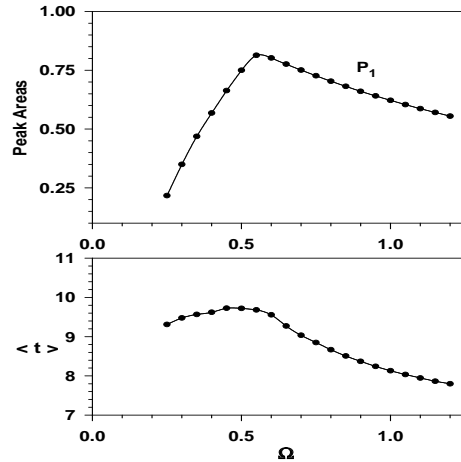


FIG. 5. Peak areas as a function of Ω and MFPT $\langle t \rangle$ as a function of Ω .

In a similar manner, for a fixed $(D/|V_0| = 1.9)$, the normalised FPTDF $g(t)$ are plotted for different signal frequencies in Fig.4. It also shows peak structure over the background. As frequency increases the

peaks are more dominant and for a given frequency peak heights fall exponentially with time. Peaks are separated by the period T_0 of the signal. After subtracting the exponential background, the peak area of the first peak (which is the most dominant) is plotted as a function of frequency of the signal in Fig.5. It also exhibits the non-monotonous behaviour. The curve shows that the synchronization (defining the strength of the synchronization as the area of the peak) is maximum at specific value of the signal frequency.

The non-monotonous behaviour of the peak strength as a function of noise strength or frequency clearly indicates that the cooperation between noise and signal becomes maximum at specific value of noise strength for given frequency or at specific value of signal frequency for given noise strength. This is the resonant behaviour in accordance with our usual convention. Thus this specific value of noise strength and signal frequency are denoted as D_{res}, Ω_{res} respectively.

As MFPT $\langle t \rangle$ is a very important time scale in this noise induced transition, we also plot $\langle t \rangle$ after evaluating them from Eq.(13) as a function of $(D/|V_0|)$ in Fig.3 and as a function of signal frequency Ω in Fig.5. For the sake of comparison MFPT when there is no signal ($A = 0$), is also plotted as a function of $(D/|V_0|)$ in Fig.3. The curves show a monotonous fall as noise strength or frequency increases except a little curb at low frequency.

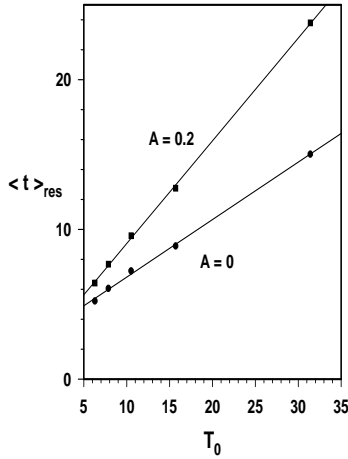


FIG. 6. MFPT at resonance $\langle t \rangle_{res}$ as a function of period of the signal T_0 with signal ($A = 0.2$) [line with filled squares] and without signal ($A = 0$) [line with filled circles].

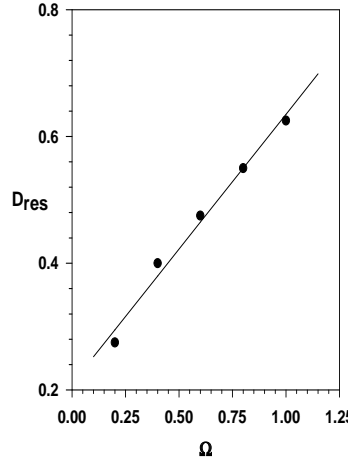


FIG. 7. Noise strength at resonance D_{res} as a function of frequency Ω

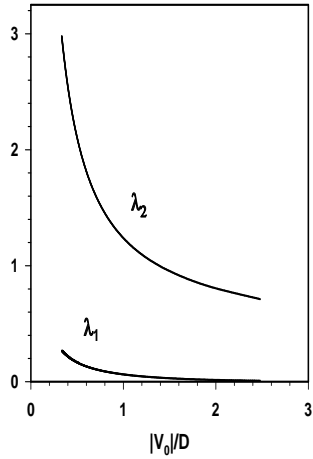


FIG. 8. Eigenvalues λ_1 and λ_2 as a function of $(|V_0|/D)$

From the resonance values $(D_{res}/|V_0|)$ (for the first dominant peak) for different frequencies $\Omega = 0.2, 0.4, 0.6, 0.8, 1.0$, we evaluate MFPT $\langle t \rangle_{res}$ from Fig.3 and plot as a function of period T_0 of the signal in Fig.6. The points fit a straight line $\langle t \rangle_{res} = .686T_0 + 2.2$. In order to have a comparison with MFPT for these resonant values $(D_{res}/|V_0|)$ for non-biased process ($A = 0$), these values are also plotted as a function of the period T_0 of the signal in the same Fig.6. They also fit straightline $\langle t \rangle_{res} = .384T_0 + 2.985$. This figure shows that as period of the signal increases the resonant time scale increases exactly in a linear fashion.

We have seen that synchronization is maximum for specific noise strengths D_{res} for different signal frequencies Ω . With these resonant values, D_{res} is plotted as a function of signal frequency Ω in Fig.7. The curve is fitted to a straight line $[D_{res} = .425\Omega + .21]$, which shows that as frequency increases the noise strength for which resonance occurs also should increase linearly.

In conclusion, we analyse the stochastic synchronization in two-state spatially extended system under the influence of periodic field analytically. The analytic expression of the conditional probability could very well exhibit the resonance behaviour and synchronization between noise and periodic signal. The expression can be further approximated with only the first term in the summation by noting that the second and consequently second onward eigenvalues (as the eigenvalues are ordered) differ from it by a large amount. The eigenvalues λ_1, λ_2 are plotted as a function of $(|V_0|/D)$ in Fig.8. The figure clearly shows that for a very large variation of the noise strength this approximation is fairly accurate.

In asymptotic expansion as given in Eq.(3) we consider only the first term. From Eq.(5b) one can estimate the magnitude of f_1 by expanding $\psi_r(x)f_1^{(r)}$ in the complete set of eigenfunctions $\{\psi_n(x)\}$ at each time t .

It can be shown that f_1 would be a periodic function and independent of position x . In fact, $f_1^{(r)}(t) \sim \Omega \text{Im}[e^{i\Omega t}/(\lambda_r + i\Omega)]$ and consequently $|f_1^{(r)}(t)| < \frac{1}{[1+(\lambda_r/\Omega)^2]^{1/2}} < 1$. Thus for small (A/D) the approximation (7) is fairly good.

The process (1) has in built scaling properties. When we change time as $t \rightarrow Dt$, $|V_0|$ would change to $(|V_0|/D)$, $\Omega \rightarrow (\Omega/D)$, $A \rightarrow (A/D)$ respectively.

The MFPT of the process at resonance is shown to increase linearly with the period of the signal. The resonant noise strength is also shown to increase linearly with frequency of the signal. This fact might help the experimentalists in studying the resonance behaviour in complex systems where tuning the frequency is a convenient task than varying the internal noise or temperature.

- [1] F. Moss, A. Bulsara, and M. Schlesinger, *Proceedings of the NATO Advanced Research Workshop on Stochastic Resonance in Physics and Biology*[J. Stat. Phys. **70** (1/2) (1993)].
- [2] L. Gammaitoni, P. Hanggi, P. Jung, and F. Marchesoni, Rev. Mod. Phys. **70**, 223 (1998).
- [3] M. Grifoni and P. Hanggi, Phys. Rep. **304**, 229 (1998).
- [4] B. Macnamara and K. Wisenfeld, Phys. Rev. **A39**, 4854 (1989).
- [5] R. F. Fox, Phys. Rev. **A39**, 4148 (1989).
- [6] P. Jung and P. Hanggi, Phys. Rev. **A44**, 8032 (1991).
- [7] T. Zhou, F. Moss, and P. Jung, Phys. Rev. **A42**, 3161 (1990).
- [8] R. F. Fox and Y. Lu, Phys. Rev. **E48**, 3390 (1993).
- [9] R. Benzi, G. Parisi, A. Sutera, and A. Vulpiani, Tellus **34**, 10 (1982).
- [10] L. Gammaitoni, F. Marchesoni, and S. Santucci, Phys. Rev. Lett. **74**, 1052 (1995).
- [11] G. Giacomelli, F. Marin, I. Rabbiosi, Phys. Rev. Lett. **82**, 675 (1999).
- [12] V. Berdichevsky and M. Gitterman, Phys. Rev. **E59**, R9 (1999).